Transition from Steric to Electrostatic Stabilization in Shell-Degradable Waterborne Particles Obtained by Photopolymerization-Induced Self-Assembly

Lei Lei, Naganatha Patil, Agathe Arnoux, Clémence Le Coeur, Yoann de Rancourt de Mimérand, Daniel Grande, Benjamin Le Droumaguet, Xiaoshuang Feng, Yves Gnanou, Benoit Couturaud

Transition From Steric To Electrostatic Stabilization in Shell-Degradable Waterborne Particles Obtained by photo-PISA

Lei Lei,[a] Naganatha Patil,[b] Agathe Arnoux,[a] Clémence Le Cœur,[a,c] Yoann de Rancourt de Mimérand,[d] Daniel Grande,[e] Benjamin Le Droumaguet,[a] Xiaoshuang Feng,[b] Yves Gnanou,[b] Benoit Couturaud*[a]*

ABSTRACT: Semi-degradable nanoparticles were synthesized in aqueous medium by photo-initiated polymerization-induced self-assembly (photo-PISA), using a cleavable hydrophilic copolymer as steric stabilizer that also served as macromolecular chain-transfer agent (mCTA) for the reversible addition-fragmentation chain transfer (RAFT) polymerization of 2-hydroxypropyl methacrylate (HPMA). This mCTA was obtained by modification of a pH-sensitive poly[(ethylene carbonate)-*co*-(ethylene oxide)] (PECEO) random copolymer that was end-fitted with a trithiocarbonate moiety. By adjusting the degree of polymerization of HPMA through RAFT, we achieved the synthesis of a series of amphiphilic block copolymers which self-assembled in various morphologies, including spheres, worms and vesicles. Through the characterization by ^{1}H-NMR, size exclusion chromatography (SEC) and transmission electron microscopy (TEM), it could be demonstrated

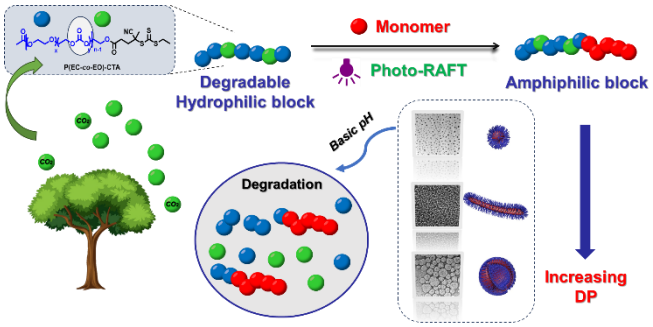

that the carbonate linkages of their hydrophilic block and of their steric stabilizer undergo hydrolysis under alkaline conditions. The length of the PHPMA block and the balance between the hydrophilic and hydrophobic blocks are two parameters that have a significant impact on the self-assembly of these particles; a transition from steric to electrostatic stabilization of these nanoparticles could be witnessed during degradation for short PHPMA blocks. In summary, pH-sensitive nanoparticles sterically stabilized by degradable poly(ether-co-ether carbonate) copolymers gave rise under basic conditions to nanoparticles stabilized by electrostatic interaction.

Introduction

Ever since the term "macromolecule" was coined in 1920 [1], a host of polymeric products now meet modern requirements for a wide range of applications, spanning from commodity polymers for food packaging [2] [3] to high value polymers for healthcare materials and others [4] [5] [6]. In most of these applications, the polymers used are made of linear arrangements of C-C bonds that are very stable but lack (bio)degradability, which in turn causes damage to the environment in addition to being responsible for large greenhouse footprint [7]. As a result, research on degradable polymers have come into focus. Various heteroatom-containing groups have thus been incorporated into polymer main chains, such as polyorthoesters [8] [9] [10], polyketone [11], polyesters [12] [13] and polycarbonates [14] [15], in order to endow the latter chains with degradability. For example, Galanopoulo *et al.* [16] recently reported the synthesis of core-degradable particles comprising polystyrene (PS) or poly(n-butyl acrylate) (PBA) and dibenzo[c, e]oxepane-5-thione (DOT) that were grown *via* RAFT-mediated PISA polymerization. They took advantage of the contribution of Gutekunst's group [17] who showed that DOT can randomly be introduced by radical means into vinylic polymers, which could be subsequently degraded by hydrolysis of their thioester-ester linkages. Previously, cyclic ketene acetals (CKAs) were also shown to afford ester-containing degradable vinylic polymers but they were difficult to handle in aqueous dispersion polymerization because of the susceptibility to hydrolysis.[18] Recently, the Gillies' group presented a "click to self-immolation" strategy to construct diverse depolymerizable polymers with various trigger units [19]. The strategy was applied to polymer-polymer coupling which afforded totally depolymerizable amphiphiles.

Made of repeating ether units, poly(ethylene oxide) (PEO) is also a polymer that is not (bio)degradable although extensively used in biomedicine for its biocompatibility, water-solubility

and stealth behavior.[20] To overcome its non-degradability, various functions, such as those based on ketal [21] [22], ester [23] [24], and carbonate [15] linkages have been incorporated into the PEO backbone to confer degradability to the resulting copolymer. For instance, carbonate functions were incorporated through copolymerization of CO_2 with ethylene oxide [25].

Recently, a method describing the preparation of poly[(ethylene carbonate)-*co*-(ethylene oxide)] (PECEO) random copolymers under metal-free conditions was reported. In such copolymerizations of ethylene oxide (EO) with carbon dioxide (CO_2) the carbonate content in the copolymer formed can be fine-tuned by varying the CO_2 pressure. This approach not only imparts degradability to the PEO backbone but it also offers the possibility to generate carbonate-containing hydrophilic copolymers [26]. Such hydrophilic and yet degradable PECEO copolymers appear as ideal candidates for the study of the stabilization of waterborne particles obtained by polymerization-induced self-assembly (PISA). PISA offers an attractive and efficient method for the synthesis of copolymers with high solids content, up to 50 wt.% [27] [28]. During the PISA process, amphiphilic block copolymers self-assemble and form nanoparticles that are sterically stabilized in morphologies, such as spheres, worms, rods, vesicles [29] [30] [31] [32]. Foremost, it is possible to add during the particle synthesis stimuli-responsive moieties [33] [34] [35]. The aim of this study is to determine how such sterically stabilized particles behave when their hydrophilic shell is partially hydrolyzed under basic conditions. We seek in particular to figure out whether a transition from steric stabilization of the nanoparticles to a stabilization by electrostatic interaction can occur in alkaline media. Besides the classical PISA process which requires a thermal radical initiator [36] [37] photo-initiated polymerization-induced self-assembly (photo-PISA) has recently emerged as a method to produce nanoparticles at ambient temperature and in milder experimental conditions.[38] [39] [40].

We thus report herein the synthesis by photo-PISA of waterborne nanoparticles, using a degradable and hydrophilic PECEO-based macro CTA to grow by RAFT a poly(2-hydroxypropyl methacrylate) block (PHPMA). This PECEO-based macro CTA segment was obtained by esterification of poly[(ethylene carbonate)$_{75}$-*co*-(ethylene oxide)$_{31}$ with 4-cyano–4-(((ethylthio)carbonothioyl)thio) pentanoic acid chain transfer agent (CEPA CTA)). The influence of the solid content and of the degree of polymerization of the PHPMA block in such poly[(ethylene carbonate)$_{75}$-*co*-(ethylene oxide)$_{31}$]-*b*-poly(2-hydroxypropyl methacrylate)$_n$ (PECEO-*b*-PHPMA) on the morphologies of the nanoparticles formed was then investigated. Subsequently, the degradability of the PECEO shell of these nano-objects and their evolution in NaOH aqueous solution were further investigated using various techniques, including SEC and TEM.

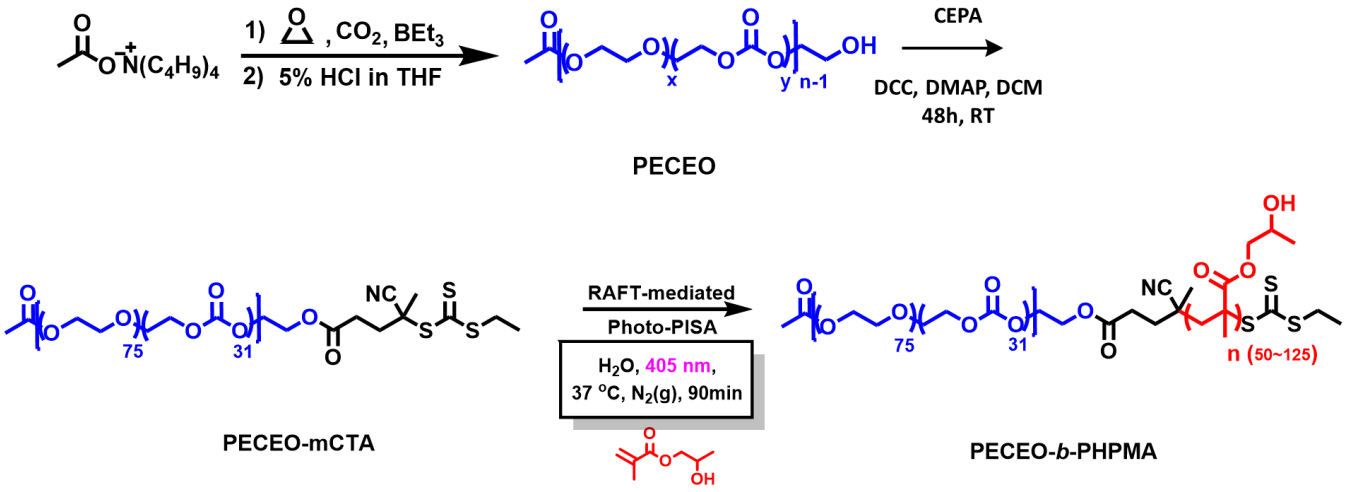

Scheme 1. Synthetic pathway for preparing PECEO-*b*-PHPMA copolymer nanoparticles with varying DP values and solids content via aqueous RAFT-mediated Photo-PISA using a degradable hydrophilic PECEO-mCTA.

Results and Discussion

Synthesis and Characterization of Hydrophilic PECEO Macro-Chain Transfer Agent (PECEO-mCTA).

The degradable PECEO block was synthesized through metal-free copolymerization of carbon dioxide (CO_2) with ethylene oxide, as reported by X. Feng *et al.* [26]. This degradable PECEO block, possessing an approximate 25 % molar content of carbonate groups was synthesized to subsequently serve as hydrophilic steric stabilizer. To this end, it was esterified with CEPA CTA to yield a hydrophilic macro-CTA. The esterification process was carried out in the presence of DCC and DMAP. A comparative analysis of ^{1}H NMR spectra of CEPA (Figure 1A), of PECEO and of PECEO-mCTA clearly demonstrates the successful functionalization of PECEO with CEPA. More specifically, all characteristic protons from CEPA could be identified on the spectra of PECEO-CEPA macro-CTA, especially the protons in α position to the carbonyl function of the ester bond formed after reaction of CEPA with PECEO at δ = 2.7 ppm together with those downshielded at δ = 1.9 and 1.3 ppm and corresponding to the C^{IV}-CH_3 terminal -CH_3 of CEPA (Figure 1), thus confirming the successful incorporation of CEPA into PECEO chain end. Furthermore, the SEC analysis of CTA-appended PECEO (M_n = 3.8 kDa) did not reveal any change in the molar mass. A negligible increase in the polymer dispersity, $Đ_M$, which rose from 1.09 to 1.16 was however observed after CEPA functionalization since PECEO chains appearing as bump or shoulder in the SEC traces are difunctional and therefore carry two CTA moieties (instead of one in monofunctional PECEO). These difunctional chains are generated by the presence of residual water in the initiator used. Additionally, M_n of PECEO-mCTA has been determined by ^{1}H-NMR (Figure S1) was 6.3 kDa. SEC measurements are done using PEO standard and do not exactly reflect the real molecular weight. Both results obtained from ^{1}H NMR spectra

and SEC analyses strongly confirm the successful synthesis of the functional degradable hydrophilic PECEO-mCTA.

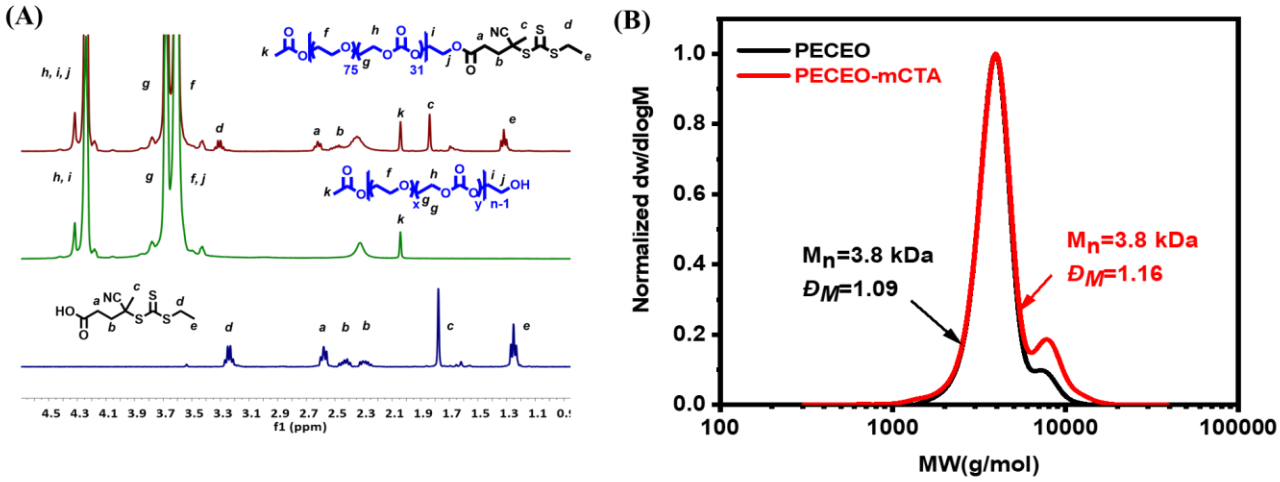

Figure 1. Pristine PECEO copolymer and PECEO-mCTA prepared through esterification (A) ^{1}H NMR spectrum of poly[(ethylene oxide)$_{75}$-*co*-(ethylene carbonate)$_{31}$] macro-CTA (PECEO-mCTA) (top), PECEO (middle) and 4-cyano-4-(((ethylthio)carbonothioyl)thio)pentanoic acid (CEPA) (bottom) in $CDCl_3$; (B) Normalized SEC RI molar mass distributions for pristine PECEO (black) and PECEO-mCTA (red).

Kinetics of Photo-PISA for PECEO-*b*-PHPMA Synthesis

The synthesized hydrophilic PECEO-mCTA was then used as a photo-iniferter to grow a PHPMA block by RAFT polymerization of HPMA through one-pot photo-PISA. HPMA was chosen because it represents a benchmark monomer for PISA. Experiments were carried out in water at 37 °C under light irradiation at 405 nm for 90 min (Scheme 1 and Table S1). The samples were withdrawn each 10 min for SEC and ^{1}H NMR analyses.

A near-quantitative HPMA conversion (98%) was achieved in 90 min. The time dependence of monomer conversion and the semilogarithmic plot associated with the PISA process are presented

in **Erreur ! Source du renvoi introuvable.**A, revealing three distinct regimes. From t = 0 to 10 min, the monomer conversion increased negligible. The relatively slow rate of reaction might be attributed to a mild retardation occurring during the polymerization of methacrylates [41]. From 10 to 40 min, monomer conversion then rose to 49 %, and the kinetics plot exhibited an apparent increase in slope, indicating the formation of molecularly dispersed copolymer chains. After this point, the conversion increased significantly to 97% monomer conversion, referring to unreacted HPMA monomer entered nascent copolymer chains to solvate the PHPMA chains, resulting in a relatively high local monomer concentration and an increased rate of polymerization [42].

A progressive molar mass increase could be observed over time, rising from 9.8 to 47.1 $kg.mol^{-1}$, while an increase in $Đ_M$ growing from 1.17 to 1.47 (Table S1). **Erreur ! Source du renvoi introuvable.**B represents this upward trend of molar mass with relatively low $Đ_M$, as determined through SEC and ^{1}H NMR analyses, in agreement with the general behavior of PISA methodology, as previously reported [43]. As shown in Figure S2. Notably, a shoulder peak could be seen towards lower molar weight values, likely due to the presence of non-functionalized PECEO-mCTA. Importantly, the SEC peak shifted towards higher molecular wight as the reaction progressed, showing a smooth molar mass increase. In general, the uniform evolution of the kinetic curve over reaction time, coupled with the consistently low $Đ_M$, provided robust confirmation of the good control achieved during the polymerization process. The observed deviation between practical M_n (determined by SEC) and theoretical line of M_n (determined by ^{1}H NMR) at high conversion is not unexpected, as the molecular weights are measured against PEO calibration.

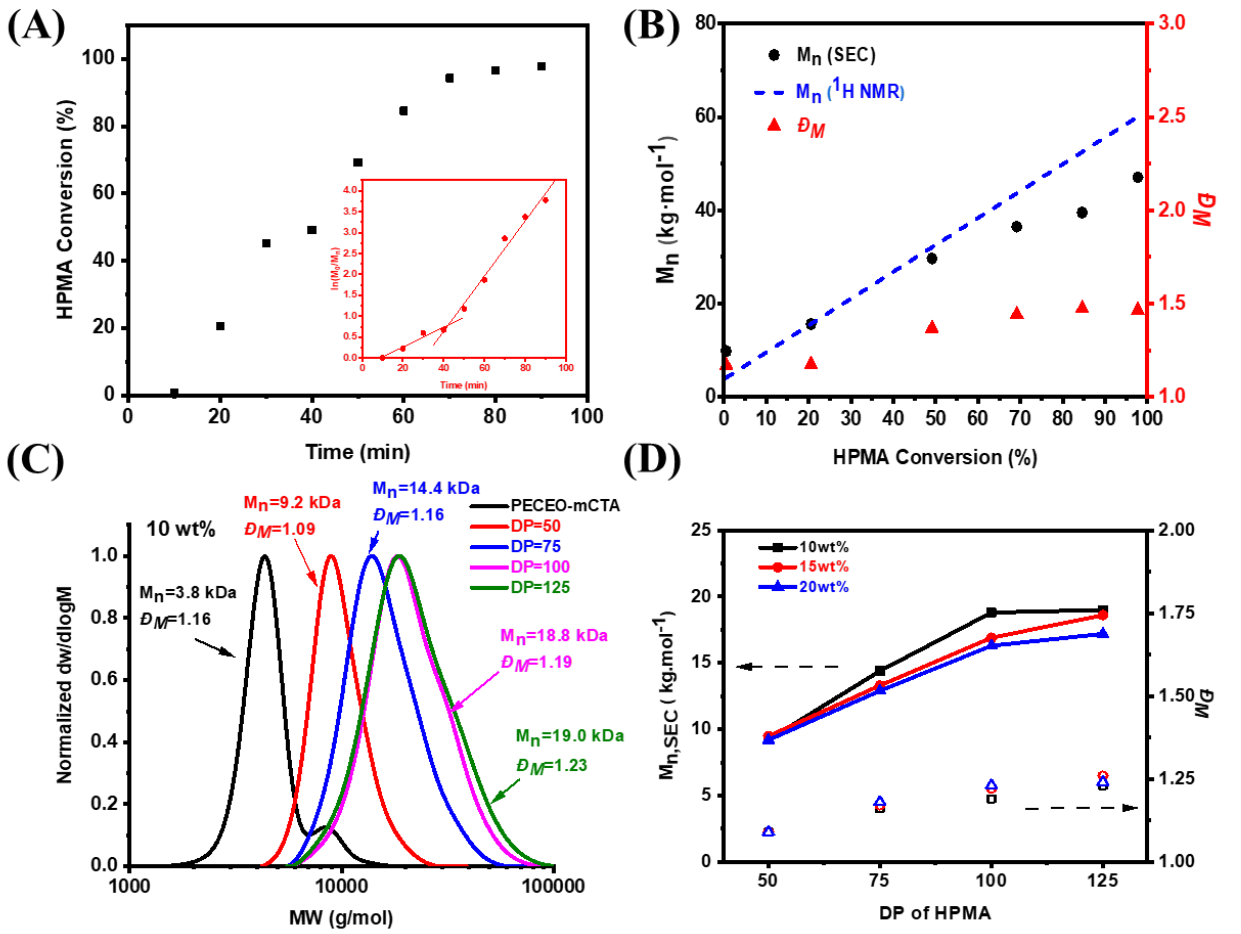

Figure 2. RAFT-mediated Photo-PISA of PECEO-*b*-PHPMA nanoparticles at DP = 100, solids content = 10 wt.% at 37 °C under light irradiation; (A) HPMA conversion and corresponding kinetics plot vs time for PECEO-*b*-PHPMA synthesis during a 90 min polymerization; (B) Evolution of M_n and $Đ_M$ vs. HPMA conversion for PECEO-*b*-PHPMA nanoparticles; (C) Normalized SEC RI traces of PECEO-mCTA and corresponding PECEO-*b*-PHPMA copolymers at 10 wt.% solids content with varying DP values (50, 75, 100, 125) showing their molar mass distribution $Đ_M$ and their M_n; (D) $M_{n,\ SEC}$ and $Đ_M$ for PECEO-*b*-PHPMA nano-objects with increasing DP values at a solids content equal to 10, 15, and 20 wt.%.

Impact of Degree of Polymerization (DP) and Solids Content on PECEO-*b*-PHPMA Nanoparticles

A series of PECEO-*b*-PHPMA diblock copolymers with varying HPMA degrees of polymerization (50, 75, 100, 125) and solid contents (10, 15, 20 wt.%) were then synthesized with a view to investigating the properties of nanoparticles in terms of morphology, size, and zeta

potential, under constant photo-polymerization conditions (37 °C, light irradiation at 405 nm) with a total reaction time of 90 min. In all cases, the final PECEO-*b*-PHPMA nanoparticles achieved a minimum monomer conversion of 68%, as determined by ^{1}H NMR spectra in DMSO-d_6 (Table S2). After dilution of the nanoparticles in water, dispersions were subjected for Dynamic Light Scattering (DLS) and zeta potential analyses.

It was observed that only PECEO-*b*-PHPMA copolymers with a DP=50 exhibited an oily phase with good flowability. The viscosity of these oily phases increased as the solids content rose from 10 to 20 wt.%. In contrast, all samples with DP values higher than 50 (75, 100, 125) aggregated to form gels, since a higher monomer concentration led to a stronger intermolecular force promoting aggregation. In all cases with the same solids content, monomodal molar mass distributions were observed, and a uniform shift towards higher mass values was found as the degree of polymerization (DP) increased from 50 to 125, maintaining a relatively narrow $Đ_M \leq 1.26$ (**Erreur ! Source du renvoi introuvable.**C and Figure S3). The small shoulder peak observed in some cases can be attributed to the formation of difunctional chains generated by the presence of residual water present in the initiator. As for the small shoulder peak seen in Figure S4, it can be attributed to non-functionalized PECEO copolymer chains. However, as it had no impact on the overall polymerization of HPMA, it was not considered in the calculation of M_n and $Đ_M$ of PECEO-*b*-PHPMA copolymers [44]. As shown in Table S2, the variation in solids content did not have a significant impact on M_n values of PECEO-*b*-PHPMA nanoparticles. Moreover, all the nanoparticles with target DP = 50 exhibited a quite narrow $Đ_M$ of 1.09. An overall increase in $Đ_M$ of synthesized PECEO-*b*-PHPMA nanoparticles was observed when either the total solids content or the polymerization degree increased (Figure 2D). This trend in the progression of M_n and $Đ_M$ values was in good agreement with the typical characteristics of the PISA procedure. Furthermore, the zeta-potential results indicated that all nano-objects derived from PECEO-*b*-PHPMA exhibited

negative charges ranging from -9.5 to -22.3 mV (Table S2). The negative surface charge of nanoparticles might be attributed to the presence of PEO-rich corona in the particles, similar negative surface charges of PEO-enrich particles were also reported by other groups[45].

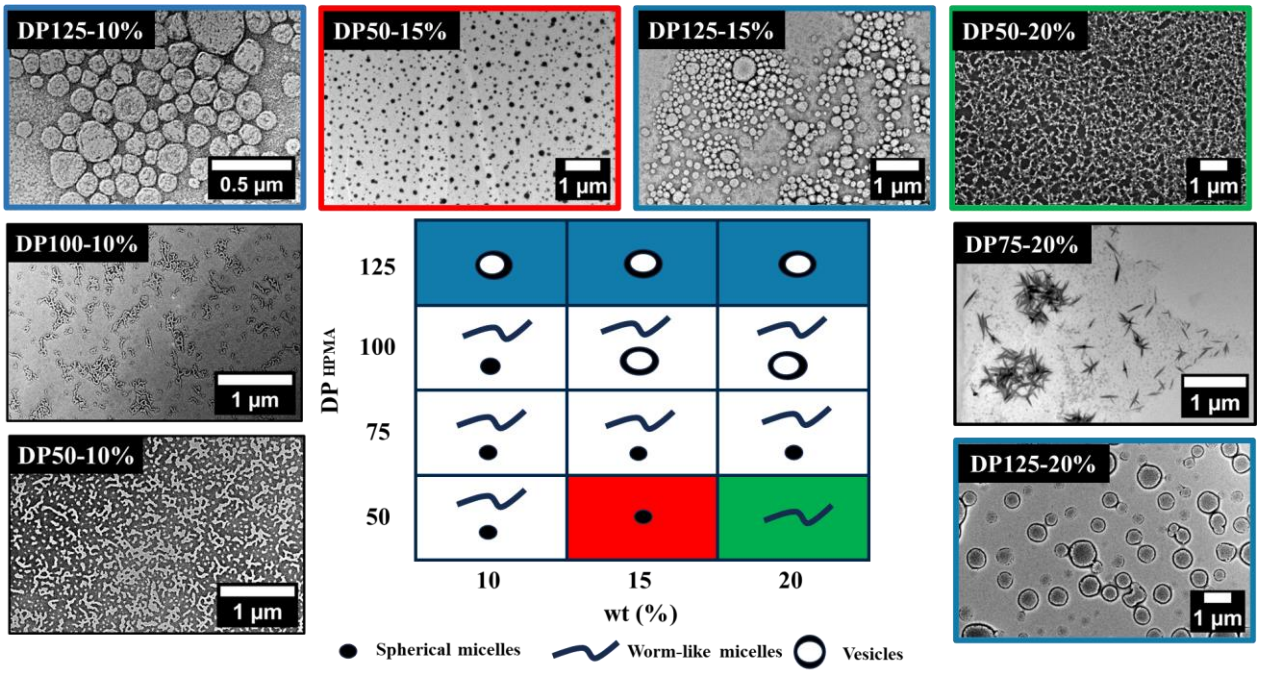

Figure 3. TEM micrographs of PECEO-*b*-PHPMA diblock copolymer nano-objects obtained upon PISA in the presence of HPMA monomer and corresponding phase diagram as a function of DP and solids content.

Dry state TEM micrographs and Figure S5-S11) along with measurements of hydrodynamic diameter and zeta potential (Table S2) were also used for analysis of PECEO-*b*-PHPMA nanoparticles with DP and solids content values ranging from 50 to 125 and from 10 to 20 wt.%, respectively; this afforded a morphology phase diagram that could be used as a guide for reproducing such synthesis. The coexistence of different nano-objects, including spherical micelles (S) and worm-like micelles (W), was observed for a DP of 50 and a 10 wt.% solids content, displaying a hydrodynamic diameter (D_h) of 121 nm and a low PDI (0.11). An increase in the solids

content up to 15 wt.% allowed the sole formation of pure spherical micelles. Finally, pure worm-like micelles were observed by TEM for 20 wt.% solids content, which confirmed that higher solids contents were conducive to achieving higher order morphologies. For DP values of 75 and 100, mixed morphologies featuring various combinations of S, W, and V were obtained, together with hydrodynamic diameters of the nano-objects ranging from 87 to 264 nm and narrow PDI between 0.11 and 0.29. Among them, a surprising coexistence of spherical micelles and needle-like structure was observed for DP = 75, and a solids content of 20 wt.%. This peculiar self-assembled nano-objects were already observed in previous research carried out in our group [28], indicative of a transition state between micelles and worm-like structures. When increasing the DP of HPMA to 125, only pure vesicle morphologies were obtained, with D_h varying from 162 to 189 nm and a PDI within the 0.21-0.27 range for 10, 15, and 20 wt.% solids content. As a conclusion, in the presence of high monomer concentrations and/or solid contents, inter-sphere fusion occurred more frequently. Moreover, the excess monomer acted as a co-solvent, efficiently solvating the PHPMA block. This solvation process proved to be advantageous for the formation of higher order morphologies.

Small-Angle Neutron Scattering (SANS) spectra of PECEO-*b*-PHPMA nanoparticles with a DP of 50 and 125 for the PHPMA block at 15 wt.% solids content are presented in Figure 4B. SANS spectra were fitted by SASview software [46] by a so-called "polymer micelle model" or "vesicle model" corresponding to a dense core with a polymeric shell and a polymeric vesicle with water-core respectively (models are detailed in SI). SANS analyses confirmed that the obtained particles had a high stability and were hard core-polymeric shell sphere, as their curves fitted perfectly to the model. Diameters measured by SANS are summarized in Table S3. There was a slight difference with results obtained in DLS and TEM measurements (Figure 4A). TEM images are a projection of the dry state of spherical objects on the focal plane and polymers grafted on the

polymer core could hardly be seen whereas DLS measures the average hydrodynamic diameters, including the water layers associated with particle surfaces. SANS assesses the static colloidal by

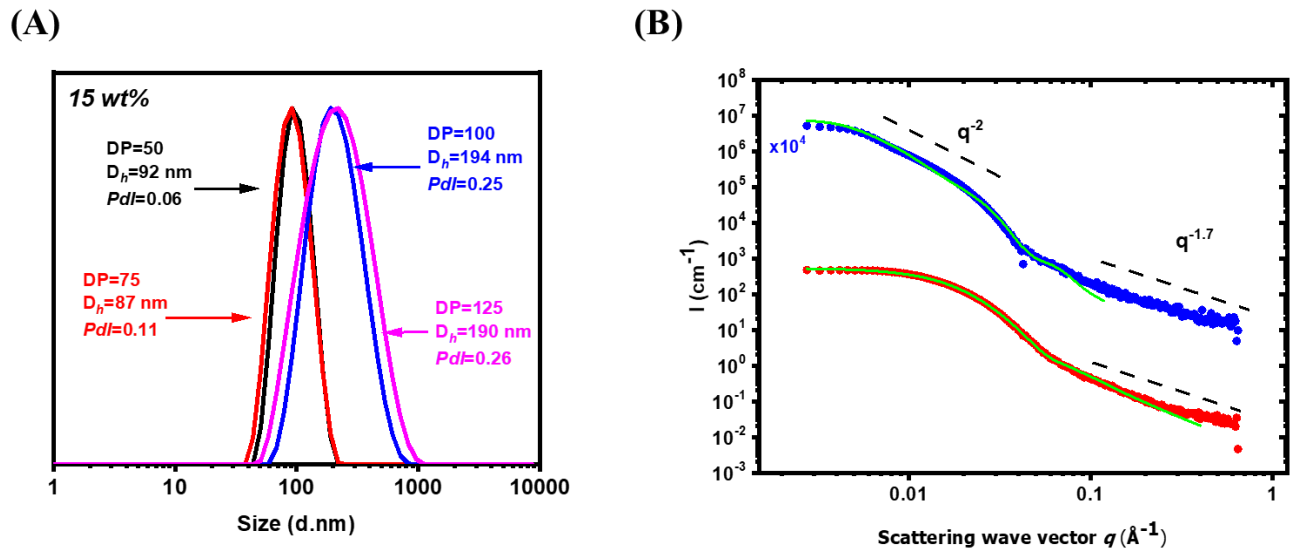

Figure 4. (A) Normalized DLS size distribution curve; (B) SANS patterns for sample DP125-15 (blue solid dot), DP50-15 (red solid dot). Green solid lines show the data fits obtained for each SANS pattern using an appropriate spherical micelle or vesicle model.

measuring the internal core size distribution of particles and excluding the external water conjugation layer. As a result, the hydrodynamic radius of polymeric objects is always higher than the radius of gyration which could account for the differences observed. For both samples, the divergence between both techniques is due to differences of size measurements. In addition, the model does not take into account in the case of vesicles the polymeric layer tethered at the surface of the vesicle which can swell into water.

Degradability of PECEO-*b*-PHPMA Copolymer Nanoparticles in Alkaline Media

In order to explore the effect of the degradation of the PECEO block on the behaviour of PECEO-*b*-PHPMA nanoparticles in basic aqueous medium, we submitted a sample of the PECEO-

b-PHPMA diblock copolymer (DP of PHPMA block = 75, solids content = 15 wt %, and total M_n = 13.3 kg.mol^{-1}) to hydrolysis. In comparison to the ^{1}H NMR spectrum of the initial PECEO-*b*-PHPMA copolymer, the one obtained after hydrolysis in 0.1 M NaOH solution (pH= 13) for overnight showed the disappearance of the peaks ascribed to the methylene protons of carbonate repeating units at 3.6 ppm and 4.17 ppm, suggesting that the latter experienced a complete degradation all along the copolymer backbone in such alkaline conditions (Figure 5B). This finding was in accordance with previous studies from Jia *et al.* on PECEO copolymers [26]. Very importantly, this also demonstrated that after hydrolysis, a remaining PEO block (located at range from 3.5-3.69 ppm) was still in polymer structures, which might link to that of PHPMA after incubating in 0.1 M NaOH solution (pH=13) (it will be proved by SEC result). Concomitantly, a significant shift of the SEC trace towards lower molar mass values, from 13.3 to 7.0 kg.mol^{-1} could be seen along with a slight decrease in the $Đ_M$ (from 1.17 to 1.14, Figure 5C). More importantly, the single SEC peak observed after degradation provides compelling evidence that the ester bond between the hydrophilic segment and the CTA remains intact. In the subsequent experiments, three PECEO-*b*-PHPMA samples with different PHPMA chain lengths but identical solids content (DP = 50, 75 and 125, at a fixed solids content of 15 wt.%) were subjected to hydrolysis (incubation in 0.01 M aqueous NaOH (pH = 12 for 12 h) and the variation of their hydrodynamic size was monitored during the degradation (**Erreur ! Source du renvoi introuvable.**A). For the DP = 50 sample, D_h increased from 92 nm to 335 nm within the first 2 h and then further reduced to 131 nm during the following 8h. A similar trend was observed for the DP = 125 sample, whose D_h increased from 190 nm to 361 nm in the initial 2 h, and then to 243 nm during the subsequent 8 h. The same decreasing trend in D_h was noticed for PECEO-*b*-PHPMA nanoparticle samples with a DP = 75 for their PHPMA block: their D_h indeed increased from 87 nm to 509 nm in the first 2 h and then dropped to 377 nm in the remaining monitoring time. In the first 2 hours of incubation, an increase

in particles' size was observed which is probably due to the enhance in hydration of the particles in NaOH 0.1M. The decline in D_h indicated that the nanoparticles disassembled after it reached a

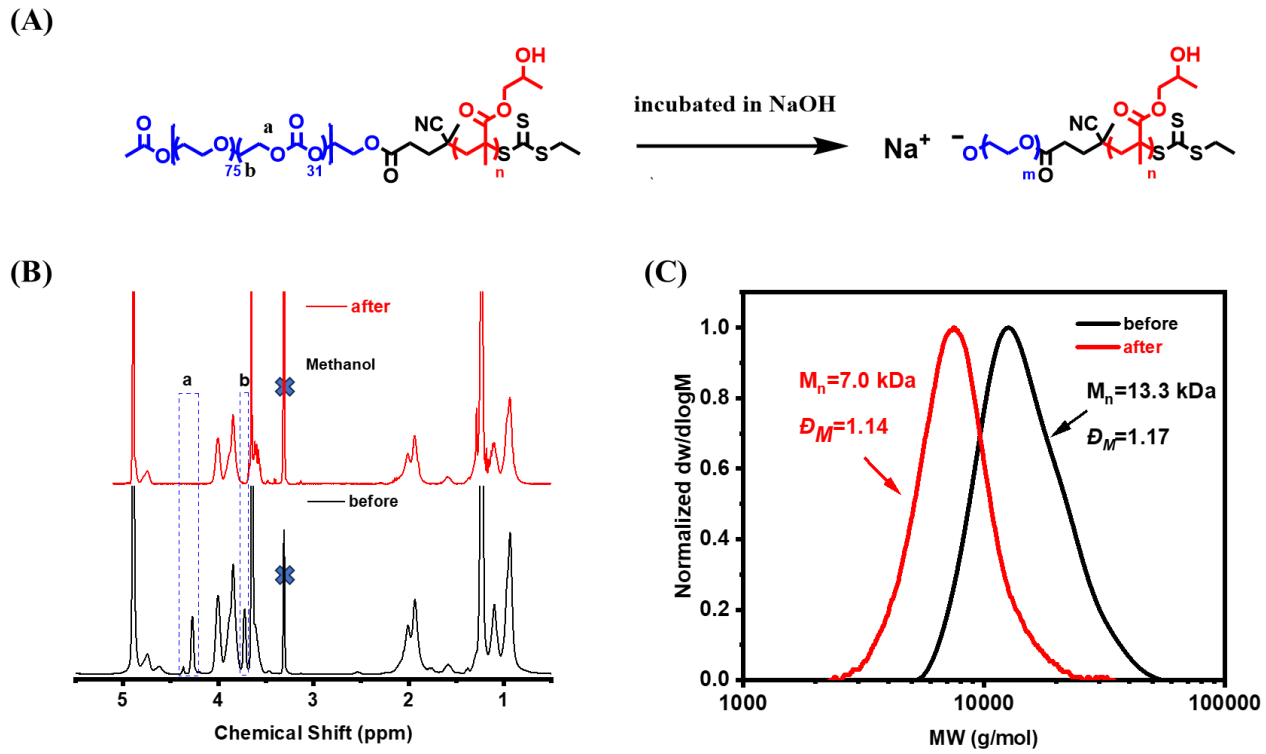

Figure 5. (A) Hypothesis for chematic illustration of the degradation of PECEO-*b*-PHPMA diblock copolymer nanoparticles in aqueous NaOH solution. The analysis was achieved with a PECEO-*b*-PHPMA displaying a degree of polymerization DP of 75 and a solids content of 15 wt.%. (B) ^{1}H NMR spectra before (black) and after (red) incubation of PECEO-*b*-PHPMA diblock copolymer nanoparticles in 0.1 M NaOH for overnight. (C) Normalized SEC-RI molar mass distribution of PECEO-mCTA and PECEO-*b*-PHPMA nanoparticles (DP = 75, solids content = 15 wt.%) before and after incubation in 0.1 M NaOH aqueous solution at room temperature for overnight, along with their corresponding $Đ_M$ values.

maximum of size in aqueous NaOH medium. As illustrated in Figure 6B, based on visual observations, nanoparticles with DP = 50, although forming a turbid solution, maintained a well-dispersed state in NaOH solution even upon degradation. For the DP = 75 sample, a similar turbid solution was observed, but some precipitates could be seen at the bottom of the vial. Notably, in the case of PECEO-*b*-PHPMA nanoparticles with a DP = 125 containing significantly a longer hydrophobic PHPMA block, it could be observed that the nanoparticles tended to aggregate and form precipitates that accumulated at the bottom of the vial [47]. This suggested that the length of the PHPMA block had a significant impact on the behavior of the particles after degradation. The distinct behaviors observed in the three copolymers after degradation (especially for shorter PHPMA blocks) could be attributed to several factors. Firstly, the hydrophilic layer made of PECEO, serving as a steric stabilizer, underwent sharp "shaving" upon degradation. Consequently, only nanoparticles with shorter hydrophobic PHPMA blocks were able to maintain stability. In other words, nanoparticles with relatively short PHPMA blocks of DP = 50 were stabilized by an even shorter hydrophilic block, suggesting that a transition might occur from a steric stabilization in the initial nanoparticles to a stabilization by electrostatic interaction by terminal alkoxide anions carried by the PEO block after hydrolysis. To prove the electrostatic stability, Zeta potential measurements of three particles before and after degradation are also provided. As shown in Figure S12, the values increased significantly after incubation in NaOH medium, from -20.2 to -42.1 mV (DP50), -18.3 to -53.1 mV (DP75), and -16.6 to -51.3 mV (DP125) respectively, resulting in formation of stronger repulsive force after degradation which help to maintain the stability for nanoparticle which has shorter hydrophobic blocks (as measuring medium changing from water to basic condition, surface charge of nanoparticles before degradation has slightly differences with previous one shown in Table S3). ^{1}H NMR analysis (Figure 5B) of the copolymer recovered after

degradation also revealed the presence of a PEO fraction, as highlighted by the presence of the characteristic ethylene oxide unit peak around 3.6 ppm. This residual PEO was thus deprotonated

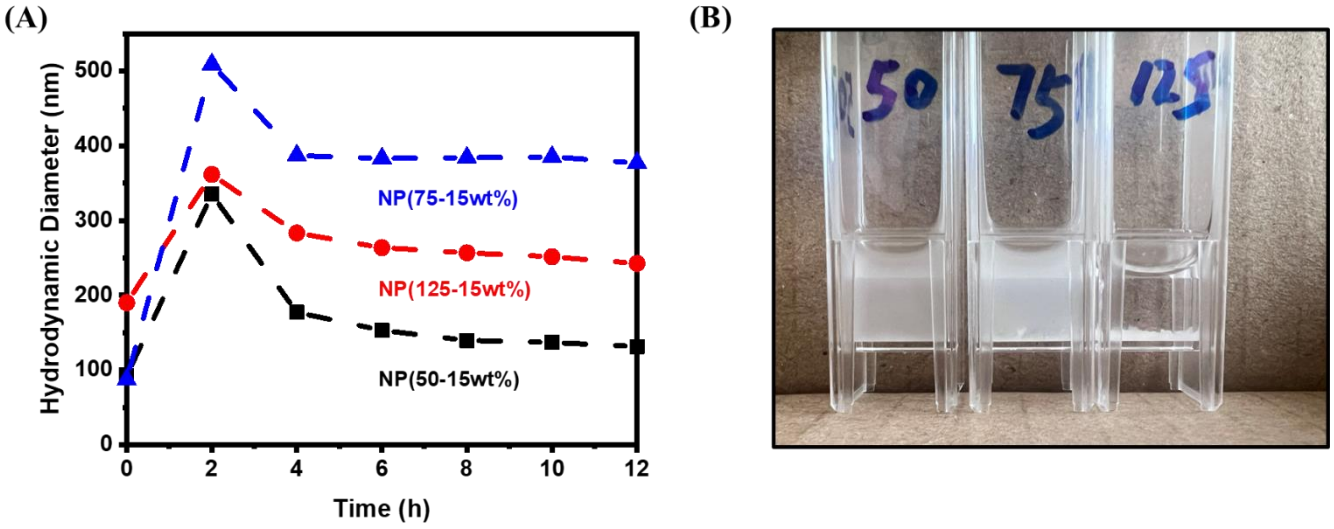

Figure 6. (A) Monitoring of hydrodynamic diameter changes of PECEO-*b*-PHPMA nanoparticles (DP = 125, solids content = 15 wt.% and DP = 50, solids content = 15 wt.%) incubated in 0.01 M NaOH aqueous solution (pH 12) at 37 °C for 12 h. (B) Physical state of PECEO-*b*-PHPMA nanoparticles at solid content of 15 wt.% with varying DP values (50, 75, 125) after 12 h incubation in NaOH medium (pH=12) at 37°C

under such alkaline conditions and end-fitted with an alkoxide anion, providing enough electrostatic repulsion to stabilize the PHPMA core of these nanoparticles.

As observed by TEM, some aggregates formed after degradation (Figure S13, B1, before; B2, after). In a enlarge figure (Figure S13, B3), it offering evidence that aggregates were formed by disassociated particles after degradation. Combining DLS results and TEM observations permitted us to conclude that the initial PECEO-*b*-PHPMA nanoparticles underwent upon hydrolysis of their hydrophilic block disruption into smaller particles, which subsequently aggregated to form larger precipitates.

Dynamic Light Scattering (DLS) results (Figure S14) of the three aforementioned samples (at DP = 50, 75, 125) that were subjected to degradation revealed a second nanoparticle population

presenting a ten-times higher diameter, after a 10-hour incubation period in 0.01 M NaOH medium (pH 12). Notably, the proportion of particles with a larger diameter increased with rising DP of the hydrophobic HPMA block. These observations could account for the differences visually observed between the samples submitted to hydrolysis and degradation of their hydrophilic block. While having identical hydrophilic blocks, nanoparticles including HPMA cores of higher DP and more hydrophobic tended to become unstable and settle as aggregates at the bottom of the vials. These findings were also confirmed by DLS measurements which actually showed a higher proportion of aggregates with higher DP. Moreover, the larger particles detected by DLS could be correlated to the aggregations observed by TEM.

Besides demonstrating that nanoparticles with short DP (= 50) of their PHPMA block and a solids content of 15 wt.% remained well-dispersed even after 10 h in 0.01 M NaOH solution (pH= 12), we incubated the same sample in different conditions (pH=7, 8, 10, 11) (Figure S15). At pH = 12 the PECEO block degraded rapidly and the sample became opaque after 10 h unlike all other samples tested at pH=7, 8, 10, 11. At pH= 12, alcoholate are formed at the end of the polymer chain which electrostatically stabilize short HPMA block.

Conclusion

A poly[(ethylene carbonate)-*co*-(ethylene oxide)] random copolymer was modified to serve as macromolecular chain transfer agent (PECEO-mCTA) for the photo-initiated RAFT polymerization of 2-hydroxypropyl methacrylate. Through polymerization-induced self-assembly (photo-PISA) waterborne could be obtained nanoparticles at ambient temperature under light irradiation. Upon monitoring the growth of the PHPMA block, we could confirm by SEC analysis of PECEO-*b*-PHPMA diblock copolymers formed that the RAFT polymerization of HPMA occurred under well-controlled conditions. A series of PECEO-*b*-PHPMA copolymers with

varying degrees of polymerization (DP) of the PHPMA block and solid contents were synthesized and the morphologies eventually obtained were characterized. The observed morphologies included spheres, worm-like micelles, and vesicles, the latter being favored as the DP of the PHPMA block and solids content increased. Subsequently, these PECEO-*b*-PHPMA-based nanoparticles were subjected to degradation through the cleavage of their carbonate groups under alkaline conditions.

Remarkably, nanoparticles with smallest hydrophobic cores remained well dispersed after partial hydrolysis of their hydrophilic outer layer, suggesting that under basic conditions their stabilization was ensured by electrostatic interaction. This versatile and efficient strategy could be envisioned as a potential synthetic platform for nanoparticle preparation and might be regarded as a potential powerful tool for designing pH-responsive systems and other related applications in the field of biomedicine.

Author Information

Corresponding Authors

Benoit Couturaud- Univ Paris Est Créteil, CNRS, Institut de Chimie et des Matériaux Paris-Est (ICMPE), UMR 7182, 2 rue Henri Dunant, 94320 Thiais, France Email: benoit.couturaud@cnrs.fr

Yves Gnanou - Physical Sciences and Engineering Division, King Abdullah University of Science and Technology (KAUST), Thuwal 23955, Kingdom of Saudi Arabia.

Email: yves.gnanou@kaust.edu.sa

Authors

Lei Lei, Benjamin Le Droumaguet, Agathe Arnoux - Univ Paris Est Créteil, CNRS, Institut de Chimie et des Matériaux Paris-Est (ICMPE), UMR 7182,2 rue Henri Dunant, 94320 Thiais, France

Naganatha Patil, Xiaoshuang Feng -Physical Sciences and Engineering Division, King Abdullah University of Science and Technology (KAUST), Thuwal 23955, Kingdom of Saudi Arabia

Clémence Le Cœur -Laboratoire Léon Brillouin, CEA-CNRS (UMR-12), CEA Saclay, Université Paris-Saclay ,91191, Gif-sur-Yvette Cedex, France

Yoann de Rancourt de Mimérand -Key Laboratory for Green Chemical Process of Ministry of Education, Wuhan Institute of Technology, Wuhan 430205, China

Daniel Grande -University of Strasbourg, CNRS, Institut Charles Sadron (ICS), UPR 22,23 rue du Loess, 67034 Strasbourg, France

Notes

The authors declare no competing financial interest.

Acknowledgements

China Scholarship Council (CSC) is thanked for funding PhD scholarship for the first author, L. LEI. The authors express their gratitude to Sylvain Prevost from Institut Laue-Langevin for his assistance with SANS experiments.

References

(1) Staudinger, H.; Ber. dtsch. Über Polymerisation. *Chem. Ges. A/B*. **1920**, 53, 1073-1085. DOI: 10.1002/cber.19200530627

(2) Zhang, M. Y.; Biesold, G. M.; Choi, W; Yu, J. Y.; Deng, L.; Silvestre, C.; Lin, Z. Q. Recent advances in polymers and polymer composites for food packaging. *Mater Today*. **2022**, 53, 134-161. DOI: 10.1016/j.mattod.2022.01.022

(3) Rhim, J. W.; Park, H. M.; Ha, C. S. Bio-nanocomposites for food packaging applications Prog. *Polym. Sci*. **2013**, 38, 1629-1652. DOI: 10.1016/j.progpolymsci.2013.05.008

(4) Xu, Y.; You, Y.; Yi, L. Y.; Wu, X. Y.; Zhao, Y. N.; Yu, J.; Liu, H.; Shen, Y.; Guo, J. M.; Huang, C. Dental plaque-inspired versatile nanosystem for caries prevention and tooth restoration. *Bioact Mater*. **2023**, 20, 418-433. DOI: 10.1016/j.bioactmat.2022.06.010

(5) Coldea, A.; Swain, M. V.; Thiel, N. Mechanical properties of polymer-infiltrated-ceramic-network materials. *Dent Mater*. **2013**, 29, 419-426. DOI: 10.1016/j.dental.2013.01.002

(6) Alqurashi, H.; Khurshid, Z.; Syed, A. U.; Habib, S. R.; Rokaya, D.; Zafar, M. S. Polyetherketoneketone (PEKK): An emerging biomaterial for oral implants and dental prostheses. *J. Adv. Res*. **2021**, 28, 87-95. DOI: 10.1016/j.jare.2020.09.004

(7) Zhang, S.; Li, R.; An, Z. Degradable Block Copolymer Nanoparticles Synthesized by Polymerization-Induced Self-Assembly. *Angew. Chem. Int. Ed*. **2023**, 63. e202315849. DOI: 10.1002/anie.202315849

(8) Bull, H. G.; Cordes, E. H. Mechanism and catalysis for hydrolysis of acetals, ketals, and ortho esters. *Chem. Rev*. **1974**, 74, 581-603. DOI: 10.1021/cr60291a004

(9) Tschan, M. J. L.; Ieong, N. S.; Todd, R.; Everson, J.; Dove, A. P. Unlocking the Potential of Poly(Ortho Ester)s: A General Catalytic Approach to the Synthesis of Surface-Erodible Materials. *Angew. Chem. Int. Ed*. **2017**, 129, 16891-16895. DOI: 10.1002/anie.201709934

(10) Binauld, S.; Stenzel, M. H. Acid-degradable polymers for drug delivery: a decade of innovation *Chem. Commun*. **2013**, 49, 2082-2102. DOI: 10.1039/c2cc36589h

(11) Arrington, K. J.; Waugh, J. B.; Radzinski, S. C.; Matson, J. B. Photo- and Biodegradable Thermoplastic Elastomers: Combining Ketone-Containing Polybutadiene with Polylactide Using Ring-Opening Polymerization and Ring-Opening Metathesis Polymerization. *Macromolecules*. **2017**, 50, 4180-4187. DOI: 10.1021/acs.macromol.7b00479

(12) Woodard, L. N.; Grunlan, M. A. Hydrolytic Degradation and Erosion of Polyester Biomaterials. *ACS Macro Lett*. **2018**, 7, 976-982. DOI: 10.1021/acsmacrolett.8b00424

(13) Nowalk, J. A.; Swisher, J. H.; Meyer, T. Y. Influence of Short-Range Scrambling of Monomer Order on the Hydrolysis Behaviors of Sequenced Degradable Polyesters *Macromolecules*. **2019**, 52, 4694-4702. DOI: 10.1021/acs.macromol.9b00480

(14) Liu, J.; Ren, W.; Lu, X. Fully degradable brush polymers with polycarbonate backbones and polylactide side chains. *Sci. China Chem*. **2015**, 58, 999-1004. DOI: 10.1007/s11426-014-5263-z

(15) Meabe, L.; Sardon, H.; Mecerreyes, D. Hydrolytically degradable poly(ethylene glycol) based polycarbonates by organocatalyzed condensation. *Eur. Polym. J*. **2017**, 95, 737-745. DOI: 10.1016/j.eurpolymj.2017.06.046

(16) Galanopoulo, P.; Gil, N.; Gigmes, D.; Lefay, C.; Guillaneuf, Y. Lages, M.; Nicolas, J.; D'Agosto, F.; Lansalot, M. RAFT-Mediated Emulsion Polymerization-Induced Self-Assembly for the Synthesis of Core-Degradable Waterborne Particles. *Angew. Chem. Int. Ed*. **2023**, 135, e202302093. DOI: 10.1002/anie.202302093

(17) Smith, R. A.; Fu, G.; McAteer, O.; Xu, M.; Gutekunst, W. R. Radical Approach to Thioester-Containing Polymers. *J. Am. Chem. Soc*. **2019**, 141, 1446-1451. DOI: 10.1021/jacs.8b12154

(18) Farmer, M. A. H.; Musa, O. M.; Armes, S. P. Efficient Synthesis of Hydrolytically Degradable Block Copolymer Nanoparticles via Reverse Sequence Polymerization-Induced Self-Assembly in Aqueous Media. *Angew. Chem. Int. Ed*. **2023**, 135, e202309526. DOI: 10.1002/anie.202309526

(19) Deng, Z.; Liang, X.; Gillies, E. R. Click to Self-immolation: A "Click" Functionalization Strategy towards Triggerable Self-Immolative Homopolymers and Block Copolymers. *Angew. Chem. Int. Ed*. **2023**, 63, e202317063. DOI: 10.1002/anie.202317063

(20) Jokerst, J. V.; Lobovkina, T.; Zare, R. N.; Gambhir, S. S. Nanoparticle PEGylation for imaging and therapy. *Nanomedicine* **2011**, 6, 715-728. DOI: 10.2217/nnm.11.19

(21) Alameda, B. M.; Murphy, J. S.; Barea-López, B. L.; Knox, K. D.; Sisemore, J. D.; Patton, D. L. Hydrolyzable Poly(β-thioether ester ketal) Thermosets via Acyclic Ketal Monomers. *Macromol. Rapid Commun*. **2022**, 43, 2200028. DOI :10.1002/marc.202200028

(22) Vrieze, J. D. ; Herck, S. Van. ; Nuhn, L. ; Geest, B. G. De. Design of pH-Degradable Polymer-Lipid Amphiphiles Using a Ketal-Functionalized RAFT Chain Transfer Agent. *Macromol. Rapid Commun*. **2020**, 41, 2000034. DOI: 10.1002/marc.202000034

(23) Iha, R. K.; Horn, B. A. Van.; Wooley, K. L.; J. Polym. Sci. Complex, degradable polyester materials via ketoxime ether-based functionalization: Amphiphilic, multifunctional graft copolymers and their resulting solution-state aggregates. Part A: *Polym. Chem*. **2010**, 48, 3553-3563. DOI: 10.1002/pola.24132

(24) Liu, D.; Bielawski, C. W. Synthesis of Degradable Poly[(Ethylene Glycol)-co-(Glycolic Acid)] via the Post-Polymerization Oxyfunctionalization of Poly(Ethylene Glycol). *Macromol. Rapid Commun*. **2016**, 37, 1587-1592. DOI: 10.1002/marc.201600336

(25) Inoue, S.; Koinuma, H.; Tsuruta, T. Makromol. *Chem*. Copolymerization of carbon dioxide and epoxide with organometallic compounds. **1969**, 130, 210-220. DOI: 10.1002/macp.1969.021300112

(26) Jia, M.; Zhang, D.; Gnanou, Y.; Feng, X. Surfactant-Emulating Amphiphilic Polycarbonates and Other Functional Polycarbonates through Metal-Free Copolymerization of CO2 with Ethylene Oxide. *ACS Sustain. Chem. Eng*. **2021**, 9, 10370-10380. DOI: 10.1021/acssuschemeng.1c03751

(27) Phan, H.; Cavanagh, R.; Destouches, D.; Vacherot, F.; Brissault, B.; Taresco, V.; Penelle, J.; Couturaud, B. H_2O_2-Responsive Nanocarriers Prepared by RAFT-Mediated

Polymerization-Induced Self-Assembly of N-(2-(Methylthio)ethyl)acrylamide for Biomedical Applications. ACS Appl. *Polym. Mater*. **2022**, 4, 7778-7789. DOI: 10.1021/acsapm.2c01327

(28) Phan, H.; Cossutta, M.; Houppe, C.; Coeur, C. L.; Prevost, S.; Cascone, I.; Courty, J.; Penelle, J.; Couturaud, B. Polymerization-Induced Self-Assembly (PISA) for in situ drug encapsulation or drug conjugation in cancer application. *J. Colloid Interface Sci*. **2022**, 618, 173-184. DOI: 10.1016/j.jcis.2022.03.044

(29) Liu, C.; Hong, C. Y.; Pan, C. Y. Polymerization techniques in polymerization-induced self-assembly (PISA). *Polym. Chem*. **2020**, 11, 3673-3689. DOI: 10.1039/d0py00455c

(30) Zhang, W. J.; Hong, C. Y.; Pan, C. Y. Polymerization-Induced Self-Assembly of Functionalized Block Copolymer Nanoparticles and Their Application in Drug Delivery. *Macromol. Rapid Commun.* **2019**, 40, 1800279. DOI: 10.1002/marc.201800279

(31) Mellot, G.; Guigner, J. M.; Bouteiller, L.; Stoffelbach, F.; Rieger, J. Templated PISA: Driving Polymerization-Induced Self-Assembly towards Fibre Morphology. *Angew. Chem. Int. Ed*. **2018**, 131, 3205-3209. DOI: 10.1002/ange.201809370

(32) Mable, C. J.; Gibson, R. R.; Prevost, S.; McKenzie, B. E.; Mykhaylyk, O. O. Loading of Silica Nanoparticles in Block Copolymer Vesicles during Polymerization-Induced Self-Assembly: Encapsulation Efficiency and Thermally Triggered Release. Armes, S. P.; *J. Am. Chem. Soc*. **2015**, 137, 16098-16108. DOI: 10.1021/jacs.5b10415

(33) Couturaud, B.; Georgiou, P. G.; Varlas, S.; Jones, J. R.; Arno, M. C.; Foster, J. C.; O'Reilly R. K. Poly(Pentafluorophenyl Methacrylate)-Based Nano-Objects Developed by Photo-PISA as Scaffolds for Post-Polymerization Functionalization. *Macromol. Rapid Commun*. **2019**, 40, 1800460. DOI: 10.1002/marc.201800460

(34) Phan, H.; Cavanagh, R.; Jacob, P.; Destouches, D.; Vacherot, F.; Brugnoli, B.; Howdle, S.; Taresco, V.; Couturaud, B. Synthesis of Multifunctional Polymersomes Prepared by Polymerization-Induced Self-Assembly. *Polymers*. **2023**, 15, 3070. DOI: 10.3390/polym15143070

(35) Phan, H.; Taresco, V.; Penelle, J.; Couturaud, B. Polymerisation-induced self-assembly (PISA) as a straightforward formulation strategy for stimuli-responsive drug delivery systems and biomaterials: recent advances. *Biomater. Sci*. **2021**, 9, 38-50. DOI: 10.1039/d0bm01406k

(36) Nguyen, D.; Huynh, V.; Lam, M.; Serelis, A.; Davey, T.; Paravagna, O.; Such, C.; Hawkett, B. Encapsulation by Directed PISA: RAFT-Based Polymer-Vesiculated Pigment for Opacity Enhancement in Paint Films. *Macromol. Rapid Commun*. **2021**, 42, 2100008. DOI: 10.1002/marc.202100008

(37) Dhiraj, H. S.; Ishizuka, F.; Elshaer, A.; Zetterlund, P. B.; Aldabbagh, F. RAFT dispersion polymerization induced self-assembly (PISA) of boronic acid-substituted acrylamides. *Polym. Chem*. **2022**, 13, 3750-3755. DOI: 10.1039/d2py00530a

(38) Yu, L.; Zhang, Y.; Dai, X.; Xu, Q.; Zhang, L.; Tan, J. Open-air preparation of cross-linked CO2-responsive polymer vesicles by enzyme-assisted photoinitiated polymerization-induced self-assembly. *Chem. Commun*. **2019**, 55, 11920-11923. DOI: 10.1039/C9CC05812E

(39) Tan, J.; He, J.; Li, X.; Xu, Q.; Huang, C.; Liu, D.; Zhang, L. Rapid synthesis of well-defined all-acrylic diblock copolymer nano-objects via alcoholic photoinitiated polymerization-induced self-assembly (photo-PISA). *Polym. Chem*. **2017**, 8, 6853-6864. DOI: 10.1039/c7py01652b

(40) Tan, J.; Bai, Y.; Zhang, X.; Huang, C.; Liu, D.; Zhang, L. Facile Preparation of CO2-Responsive Polymer Nano-Objects via Aqueous Photoinitiated Polymerization-Induced Self-Assembly (Photo-PISA). *Macromol. Rapid Commun*. **2016**, 37, 1434-1440. DOI: 10.1002/marc.201600508

(41) Blanazs, A.; Madsen, J.; Battaglia, G.; Ryan, A. J.; Armes, S. P. Mechanistic Insights for Block Copolymer Morphologies: How Do Worms Form Vesicles. *J. Am. Chem. Soc.* **2011**, 133, 16581-16587. DOI: 10.1021/ja206301a

(42) Tan, J. ; Bai, Y. ; Zhang, X. ; Zhang, L. Room temperature synthesis of poly(poly(ethylene glycol) methyl ether methacrylate)-based diblock copolymer nano-objects via Photoinitiated Polymerization-Induced Self-Assembly (Photo-PISA). *Polym. Chem.* **2016**, 7, 2372-2380. DOI: 10.1039/C6PY00022C

(43) Foster, J. C.; Varlas, S.; Couturaud, B.; Coe, Z.; O'Reilly, R. K. Getting into Shape: Reflections on a New Generation of Cylindrical Nanostructures' Self-Assembly Using Polymer Building Blocks. *J. Am. Chem. Soc.* **2019**, 141, 2742-2753. DOI: 10.1021/jacs.8b08648

(44) Varlas, S.; Georgiou, P. G.; Bilalis, P.; Jones, J. R.; Hadjichristidis, N.; O'Reilly, R. K. Poly(sarcosine)-Based Nano-Objects with Multi-Protease Resistance by Aqueous Photoinitiated Polymerization-Induced Self-Assembly (Photo-PISA). *Biomacromolecules*. **2018**, 19, 4453-4462. DOI: 10.1021/acs.biomac.8b01326

(45) Ridolfo, R.; Williams, D. S.; Hest, J. C. van. Influence of surface charge on the formulation of elongated PEG-b-PDLLA nanoparticles. *Polym. Chem.* **2020**, 11, 2775-2780. DOI: 10.1039/D0PY00280A

(46) "SasView 5.0.3 Documentation", can be found under http://www.sasview.org (accessed **2019**).

(47) Joubert, F. ; Pasparakis, G. Well - defined backbone degradable polymer – drug conjugates synthesized by reversible addition - fragmentation chain - transfer polymerization. *J. Polym. Sci*. **2020**, 58, 2010-2021. DOI : 10.1002/pol.20200303